



Ozone super recovery cancelled in the Antarctic upper stratosphere

Ville Maliniemi¹, Hilde Nesse Tyssøy¹, Christine Smith-Johnsen¹, Pavle Arsenovic², and Daniel R. Marsh^{3,4}

¹Birkeland Centre for Space Science, Department of Physics and Technology, University of Bergen, Norway

²EMPA Swiss Federal Laboratories for Material Science and Technology, Zurich, Switzerland

³National Center for Atmospheric Research, Boulder, CO, USA

⁴Faculty of Engineering and Physical Sciences, University of Leeds, UK

Correspondence: Ville Maliniemi (ville.maliniemi@uib.no)

Abstract. Ozone is expected to fully recover from the CFC-era by the end of the 21st century. Furthermore, because of anthropogenic climate change, a cooler stratosphere accelerates ozone production and is projected to lead to a super recovery of ozone. We investigate the ozone distribution over the 21st century with four different future scenarios using simulations of the Whole Atmosphere Community Climate Model (WACCM). At the end of the 21st century, equatorial upper stratosphere has roughly 0.5 to 1.0 parts per million more ozone in scenario with the highest greenhouse gas emissions compared to conservative scenario. Polar ozone levels exceed those in the pre CFC-era in scenarios that have the highest greenhouse gas emissions. This is true in the Arctic stratosphere and the Antarctic lower stratosphere. The Antarctic upper stratosphere is an exception, where different scenarios all have similar levels of ozone during winter, which do not exceed pre-CFC levels. Our results show that this is due to excess nitrogen oxides (NO_x) descending from above in the stronger scenarios of greenhouse gas emissions. NO_x is formed by energetic electron precipitation (EEP) in the thermosphere and the upper mesosphere, and descends faster through the mesosphere in stronger scenarios. This indicates that the EEP indirect effect will be important factor for the future Antarctic ozone evolution, and could potentially prevent a super recovery of ozone in the upper stratosphere.

1 Introduction

Stratospheric ozone experienced a dramatic decrease from the 1960s until the 1990s due to the human induced chloro-fluoro-carbon (CFC) emissions (Cicerone, 1987; Anderson et al., 1991) and the associated increase of reactive chlorine oxides (ClO_x) in the stratosphere. Since then, the Montreal Protocol has been able to limit the use of CFCs (Velders et al., 2007), and in the beginning of the 21st century stratospheric ozone is showing signs of recovery (Solomon et al., 2016).

Greenhouse gas emissions also alter the stratospheric ozone (Langematz, 2018). As a consequence of higher levels of carbon dioxide (CO_2), the stratosphere is cooling, which increases the rate of stratospheric ozone production (Li et al., 2009). This is projected to lead to a super recovery of ozone, i.e., a higher total ozone column than before the 1960s (WMO, 2018). In addition to the impact on chemical ozone production, climate change is modulating ozone through changes in the atmospheric circulation. The Brewer-Dobson circulation (BDC) is increasing (Garcia and Randel, 2008; Butchart, 2014) and leads to enhanced transport of ozone to high latitudes, especially from equatorial lower stratosphere (Langematz, 2018; Shepherd, 2008).



Projection of upper stratospheric meridional residual circulation differ in opposite hemispheres. As a consequence of radiative forcing increase of greenhouse gas emissions, the polar vortex is weakening in the northern hemisphere (Mitchell et al., 2012), while in the southern hemisphere it is strengthening (Thompson and Solomon, 2002). As a result, upper stratospheric meridional circulation and ozone super recovery are projected to be stronger in the northern hemisphere (WMO, 2018).

Polar stratospheric ozone is also impacted from above. Energetic electron precipitation (EEP) from the magnetosphere is able to produce reactive nitrogen oxides (NO_x) in the thermosphere and upper mesosphere (Andersson et al., 2018). The chemical lifetime of NO_x is enhanced during wintertime polar darkness allowing NO_x to be transported to the upper stratosphere with the prevailing vertical residual circulation (Randall et al., 2006; Funke et al., 2014). Recently, Maliniemi et al. (2020) showed in the Whole Atmosphere Community Climate Model (WACCM) that this EEP indirect NO_x effect will become substantially stronger during the 21st century in the southern hemisphere with higher greenhouse gas emissions. Similar results have been obtained earlier with the EMAC chemistry-climate model (Baumgaertner et al., 2010). This is a consequence of stronger mesospheric descent in the future Antarctic (Maliniemi et al., 2020), due to a strengthening of the polar vortex. No such strengthening of the EEP indirect effect is predicted in the Arctic (Maliniemi et al., 2020).

In this paper we investigate the ozone distribution over the 21st century under four different future scenarios using the WACCM chemistry-climate model. We concentrate on polar stratospheric variability during winter, but also show results over the whole atmosphere and during all seasons. Section 2 describes the data and statistical methods. Section 3 provides results divided to three subsections: the polar winter ozone evolution from pre-industrial era until the end of the 21st century; global ozone distribution at the end of the 21st century between the strongest and conservative future scenarios regarding the greenhouse gas emissions; and same for the polar ozone. Summary is given in Section 4.

2 Data and Methods

Data used in this study comes from simulations of a free-running version of the chemistry-climate model WACCM6 within CESM2. The model parameters are explained in details by Marsh et al. (2013) with updates in Gettelman et al. (2019). Five different simulations are analyzed. Historical simulations (3 ensemble members) cover the period 1850-2014 (CMIP6 (Coupled Model Intercomparison Project) DECK simulations). Four different future scenario (CMIP6 ScenarioMIP: SSP1, SSP2, SSP3 and SSP5 (Shared Socioeconomic Pathway)) simulations cover the period 2015-2100 (O'Neill et al., 2016). SSP1 and SSP3 have 1 ensemble member and SSP2 and SSP5 have 5 ensemble members. Shown results are the mean of ensemble members for historical, SSP2 and SSP5 model runs.

Different SSPs include a wide range of future actions by society, including greenhouse gas emissions. Global average CO_2 concentrations in 2100 are 446 parts per million (ppm) in SSP1, 603 ppm in SSP2, 867 ppm in SSP3 and 1135 ppm in SSP5 (Meinshausen et al., 2020). Radiative forcing increase of the climate system by 2100 relative to pre-industrial era are 5.0 W/m^2 in SSP1, 6.5 W/m^2 in SSP2, 7.2 W/m^2 in SSP3 and 8.7 W/m^2 in SSP5. Details of the different SSPs can be obtained from Riahi et al. (2017). All model runs have solar activity following the recommendations of CMIP6. This provides estimates of



the solar activity before the space era, and a future solar forcing scenario (1850-2100 in this case) (Matthes et al., 2017). All SSPs have the same future solar activity scenario (reference scenario).

We concentrate on monthly mean zonal mean volume mixing ratios of ozone, NO_x and ClO_x , as well as temperature and zonal wind. The latitudinal resolution of the model is 0.94° (192 bins) and altitude ranges from the surface up to 140 km (in 70 levels). In this study we focus on altitudes from around the mesopause to the surface (0.01 hPa to 1000 hPa). We analyse the centennial time series (1850-2100) of ozone and ClO_x concentrations in the polar stratosphere, as well as the Brewer-Dobson circulation in the equatorial stratosphere. The smooth long-term variations shown in Figures 1, 2 and 5 are calculated using the LOWESS-method (LOcally WEighted Scatterplot Smoothing) applied with a 31-year window (Cleveland and Devlin, 1988).

We subtract the SSP2 from the SSP5 to evaluate the differences in ozone (Figure 3 and 7), NO_x (Figure 6 and 7), temperature and zonal wind (Figure 4) during 2090-2100 period, i.e., $\text{SSP5}[\text{ensemble mean}] - \text{SSP2}[\text{ensemble mean}]$. Statistical significance for the differences between SSP5 and SSP2 during 2090-2100 are calculated applying a Monte Carlo method: we take a random 11-year time period from 2015-2100 and calculate the difference in each latitude/height bin. This is performed 1000 times and original value (difference in 2090-2100) is compared to the distribution of these 1000 repetitions to obtain fraction of more extreme differences (both tails of the distribution). This fraction then represents the p-value in each bin with the null hypothesis that there is no difference between SSP5 and SSP2.

In addition, we use a method proposed by Wilks (2016) called a false detection rate. This is done because our results for 2090-2100 differences are presented over several latitudes and altitudes, and thus have a multiple hypothesis testing situation. This method adjusts the p-values to take into account the spatial autocorrelation and the fact that the probability to erroneously rejecting the null hypothesis increases with the number of individual hypothesis tests. Thus, after the procedure, we obtain a global significance of 95% of the whole presented grid, which means that the probability to erroneously rejecting the (individual) null hypothesis will be 5%.

3 Results

3.1 Centennial polar winter ozone in different future scenarios

Figure 1 shows the late winter polar ozone time series for the upper and the lower stratosphere in both hemispheres. The minimum level of ozone is reached a few years after 2000 (Solomon et al., 2016). Ozone returns to 1980s level around 2050 in the southern hemisphere and a little bit earlier in the northern hemisphere. Different future scenarios start to diverge from each other after 2050. SSP3 and SSP5 go above 1960 levels towards the end of the 21st century, most notably in the northern hemisphere. The Antarctic lower stratosphere shows a super recovery in SSP3 and SSP5, but the Antarctic upper stratosphere does not.

Figure 2 shows the time series of late winter ClO_x in the Antarctic stratosphere. One can see that the maximum level of ClO_x coincides with the minimum in ozone around year 2000. After that ClO_x starts to decrease as a result of the Montreal protocol (Velders et al., 2007). All different future scenarios have approximately the same evolution of stratospheric ClO_x , following

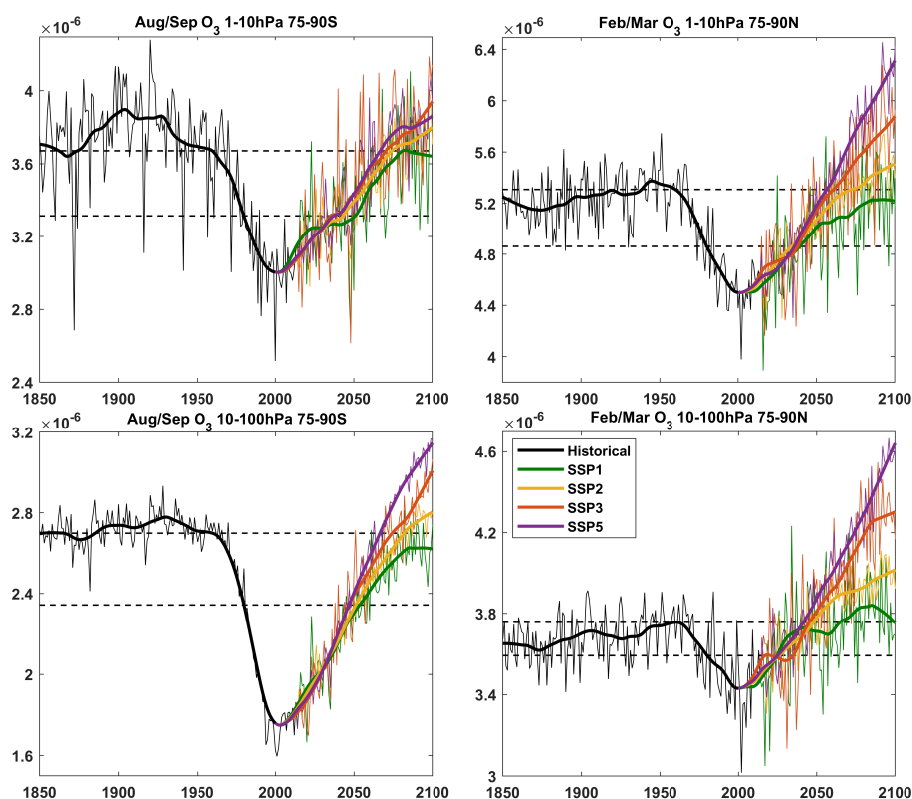


Figure 1. Time series of Antarctic upper (top left) and lower stratosphere (bottom left) Aug/Sep ozone during 1850–2100, and same for Arctic (top right: upper stratosphere, bottom right: lower stratosphere) in Feb/Mar. Values represent mean volume mixing ratios in corresponding pressure range. Black=1850–2014 historical run (mean of three ensemble members), green=2015–2100 SSP1 (one ensemble), yellow=2015–2100 SSP2 (five ensembles), red=2015–2100 SSP3 (one ensemble), and purple=2015–2100 SSP5 (five ensembles). Thin lines represent yearly average and thick lines represent 31-year smoothed trend calculated with LOWESS-method. Smoothed trends for SSPs are calculated continuously with the historical run to avoid gaps around 2015 (note the SSP thick lines starting from year 2000). Dotted lines represent average level during 1960 and 1980.

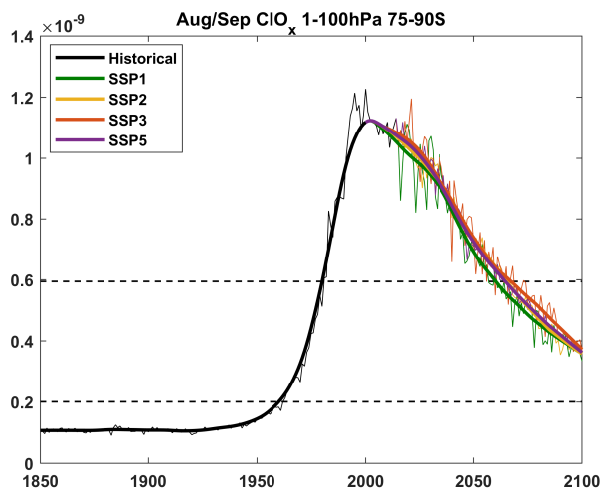


Figure 2. Same as Figure 1 for Aug/Sep ClO_x in Antarctic stratosphere (1-100 hPa).

the fact that all SSPs have the same WMO CFC-scenario (Meinshausen et al., 2020). We note that the Arctic stratosphere also obtains closely similar evolution of ClO_x in different SSPs (not shown).

90 3.2 Global ozone difference between SSP5 and SSP2 at the end of the 21st century

Figure 3 presents the difference in monthly ozone between SSP5 and SSP2 during 2090-2100. There are substantially more stratospheric ozone in SSP5 relative to SSP2. SSP5 has approximately 0.5 to 1.0 ppm more equatorial stratospheric ozone above 20 hPa in all months. However, below 20 hPa SSP5 has significantly less equatorial ozone than in SSP2 (up to -0.3 ppm). Additional feature is seen in the mesosphere where consistently lower ozone levels are obtained in SSP5 than in SSP2.

95 Note though that the negative anomalies are less than -0.1 ppm in regions other than high latitudes.

These global differences between SSP5 and SSP2 can be explained in terms of carbon dioxide and methane emissions (Kirner et al., 2015). The increased ozone in the equatorial upper stratosphere is caused by increased ozone production due to cooler future middle atmosphere. This is because of the temperature dependency of the Chapman cycle (Brasseur and Solomon, 2005). Figure 4 shows the temperature difference between SSP5 and SSP2. The temperature is between 4 to 8 K lower in SSP5
100 than in SSP2 in the upper stratosphere, with the largest differences in high latitudes during winter.

Mesospheric ozone decrease between SSP5 and SSP2 is likely a consequence of additional methane emissions in SSP5 (Riahi et al., 2017). Methane oxidation produces water vapour and hydrogen oxides (HO_x) (le Texier et al., 1988). In the mesosphere, additional production of HO_x is able to overcome the temperature effect and lead to a total negative ozone anomaly (Kirner et al., 2015).

105 Negative ozone anomalies in the equatorial lower stratosphere are mainly due to dynamical changes. Climate change has been shown to accelerate the Brewer-Dobson circulation (Garcia and Randel, 2008; Butchart, 2014) as shown for the annual

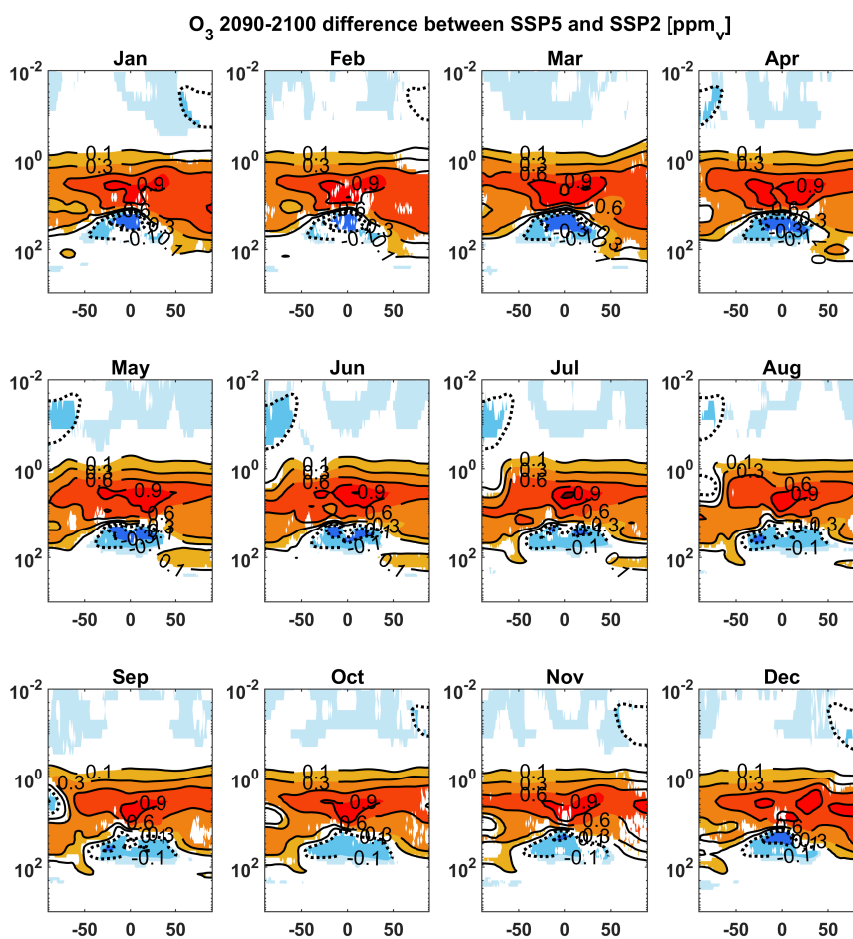


Figure 3. Monthly zonal mean ozone difference between SSP5 and SSP2 in parts per million during 2090-2100. Horizontal axes show the latitude in degrees and vertical axes the altitude in air-pressure units of hPa. Positive contour levels are 0.1, 0.3, 0.6, 0.9 and 1.2 ppm (solid lines), and negative contour levels are -0.1, -0.3 ppm (dotted lines). Colours represent areas significant with 95% calculated with a monte carlo simulation and a false detection rate.

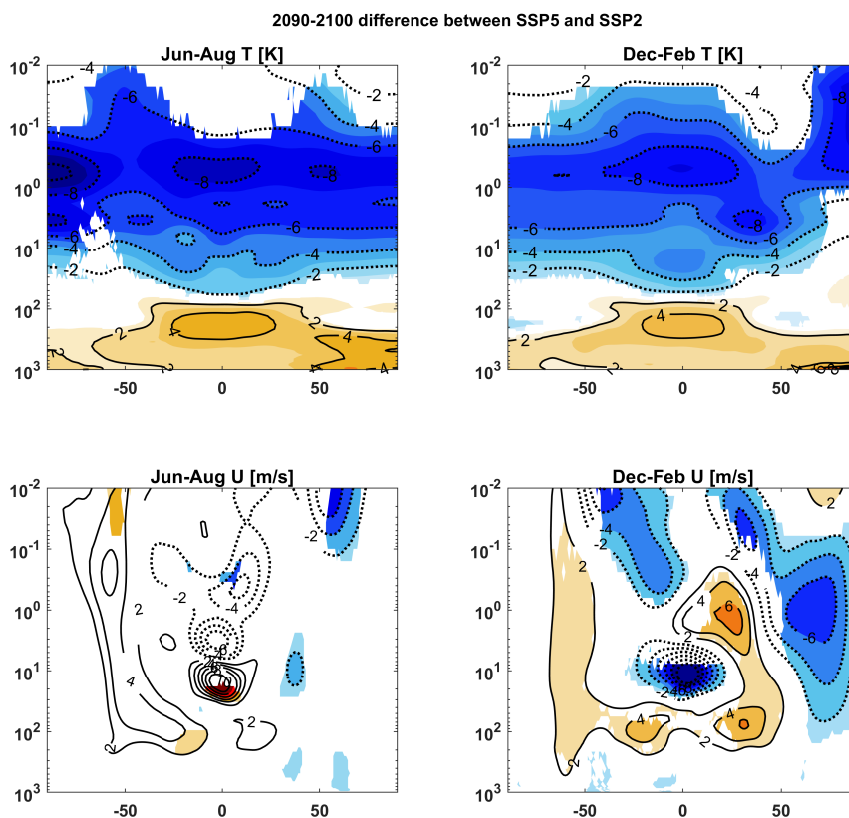


Figure 4. Zonal mean temperature (top left: Jun-Aug, top right: Dec-Feb) and zonal mean zonal wind (bottom left: Jun-Aug, bottom right: Dec-Feb) differences between SSP5 and SSP2 during 2090-2100. Horizontal axes show the latitude in degrees and vertical axes the altitude in air-pressure units of hPa. Positive contour levels are 2, 4, 6, 8 and 10 (solid lines), and negative contour levels are -2, -4, -6, -8 and -10 (dotted lines) as K for temperature and m/s for zonal wind. Colours represent areas significant with 95% calculated with a monte carlo simulation and a false detection rate.

BDC in different scenarios in Figure 5. The largest equatorial vertical residual circulation speed at the end of the 21st century occurs in SSP5, followed by SSP3, SSP2 and SSP1, respectively. This leads to enhanced transport of ozone from the lower equatorial stratosphere, resulting in a negative anomaly in SSP5 relative to SSP2 (Langematz, 2018). The ozone difference in
110 lower equatorial stratosphere between SSP5 and SSP2 could also be partly due to increased overhead ozone, which attenuates the ultraviolet radiation and decreases the photolysis of oxygen in this region (Kirner et al., 2015).

3.3 Polar ozone difference between SSP5 and SSP2 at the end of the 21st century

Figure 3 shows that the Arctic stratosphere consistently obtains more ozone in SSP5 than in SSP2, reaching highest values during winter (November to March) but this does not occur in the Antarctic stratosphere. During winter (June to September)

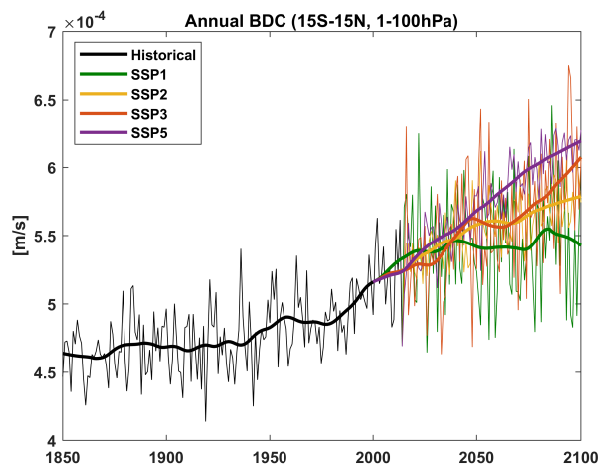


Figure 5. Time series of the annual Brewer-Dobson circulation (vertical residual circulation speed at 15°S - 15°N , 1-100hPa). Colours represent the same simulations as in Figure 1.

115 a negative ozone anomaly (in SSP5 relative to SSP2) is obtained descending from 1 hPa to 10-20 hPa. Maliniemi et al. (2020) showed that southern polar mesospheric descent rates will accelerate in the future under higher greenhouse gas forcing, and leads to more EEP indirect stratospheric NO_x . Figure 6 shows the NO_x difference between SSP5 and SSP2 in 2090-2100. Over the whole atmosphere there is slightly less NO_x in SSP5 than in SSP2. This is in line with slightly lower N_2O emissions in SSP5 than in SSP2 (Riahi et al., 2017). Cooler stratosphere also increases the chemical destruction of NO_x (Stolarski et al.,
120 2015). Additionally, one can see that there is a substantial increase of NO_x in the Antarctic mesosphere and upper stratosphere from June until September. The NO_x increase in the upper stratosphere is up to 10 parts per billion (ppb). This is more evident in Figure 7, which shows polar ozone and NO_x differences between SSP5 and SSP2 during the winter months. The altitude of the negative ozone anomaly in the Antarctic stratosphere follows the altitude of NO_x increase closely and is statistically significant during September.

125 The NO_x difference in the northern hemisphere is less dramatic. There is an increase in the upper mesosphere from November to March (see Figure 6) but it does not descend to lower altitudes. Figure 7 also shows that no polar NO_x increase occurs below 0.1 hPa during Jan-Apr, and ozone concentration in the stratosphere does not experience any dramatic variability over different winter months, as opposed to the descending negative anomaly seen in the Antarctic stratosphere.

Figure 4 shows the difference of zonal wind between SSP5 and SSP2 during southern and northern winters. The polar
130 vortex is weaker in the northern hemisphere but slightly stronger in the southern hemisphere in SSP5. A stronger polar vortex accelerates the mesospheric descent, while it weakens the mean meridional residual circulation in the upper stratosphere (not shown). This might lead to overall lower levels of ozone in the Antarctic stratosphere than in the Arctic stratosphere. However, the ozone super recovery is occurring in the Antarctic lower stratosphere (as seen in Figure 1), which implies that the excess

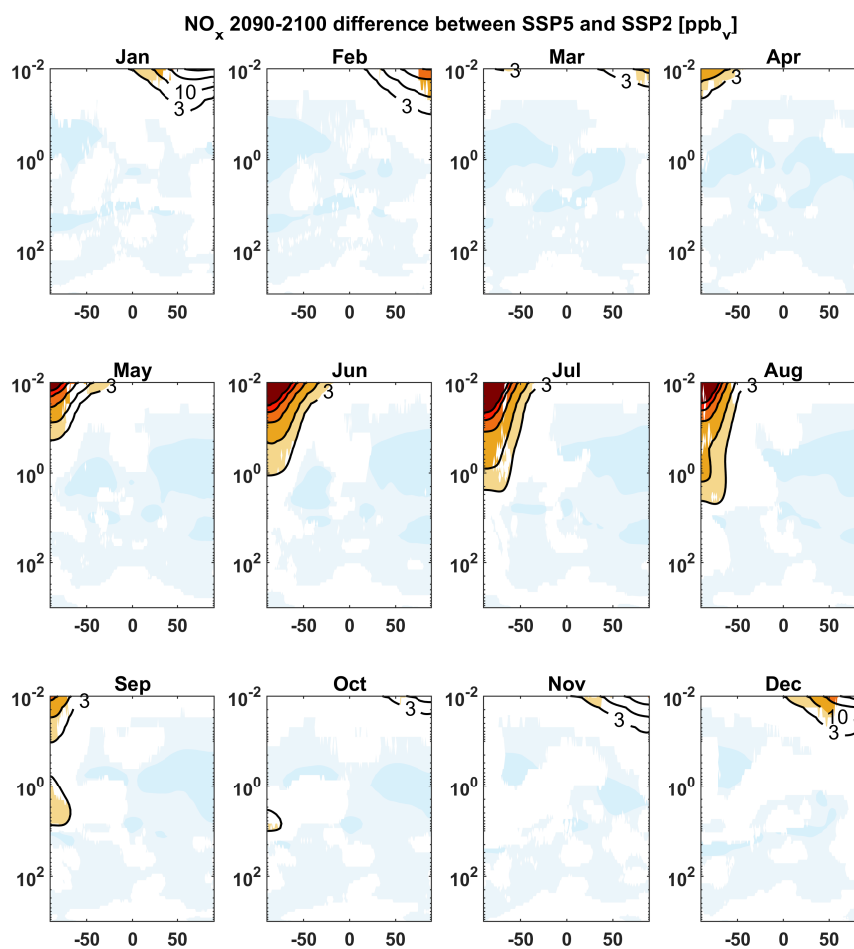


Figure 6. Monthly zonal mean NO_x difference between SSP5 and SSP2 in parts per billion during 2090-2100. Horizontal axes show the latitude in degrees and vertical axes the altitude in air-pressure units of hPa. Positive contour levels are 3, 10, 30, 60 and 90 ppb (solid lines). Colours represent areas significant with 95% calculated with a monte carlo simulation and a false detection rate. All negative responses are below -1 ppb.

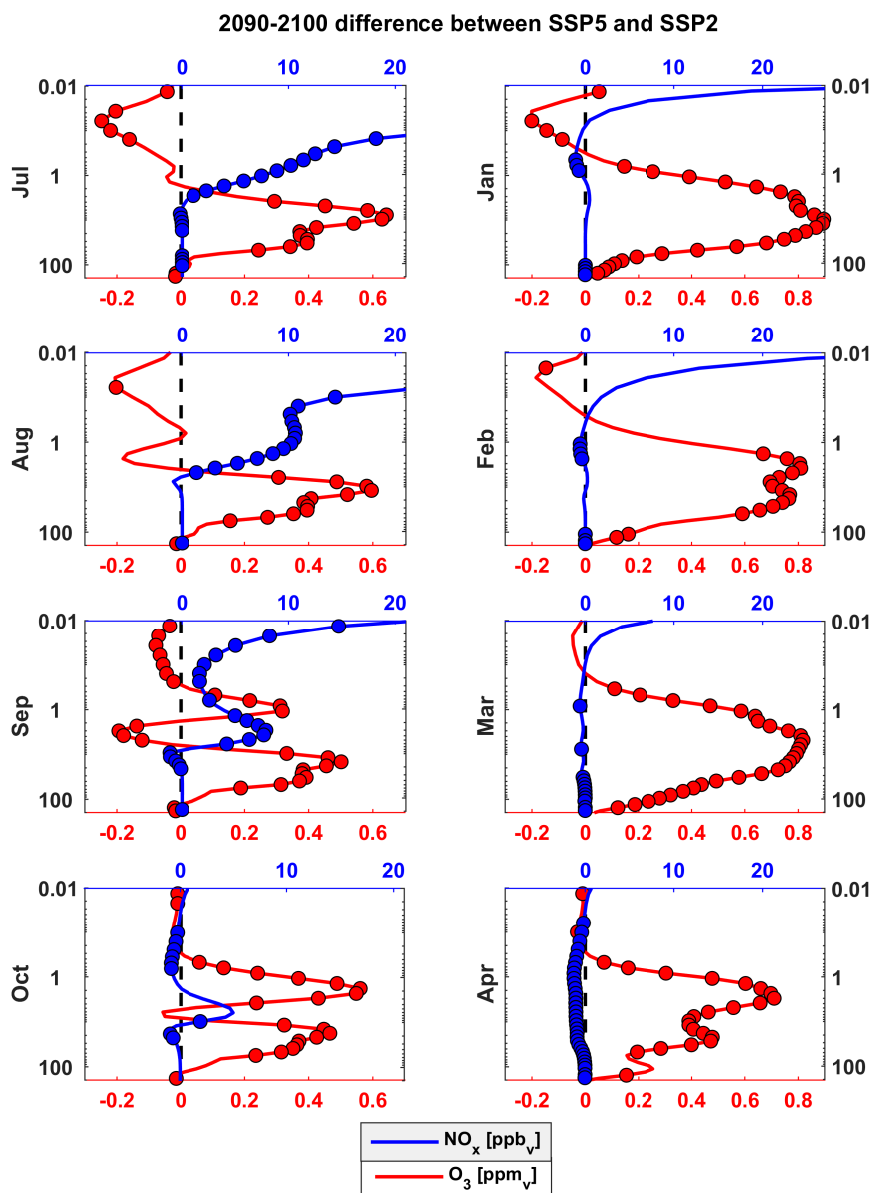


Figure 7. Monthly zonal mean polar (75-90°S during Jul-Oct and 75-90°N during Jan-Apr) NO_x (blue, parts per billion) and ozone (red, parts per million) differences between SSP5 and SSP2 during 2090-2100. Vertical axes show the altitude in air-pressure units from 0.01 to 200 hPa. Coloured circles represent values significant with 95% calculated with a monte carlo simulation and a false detection rate.



135 descending NO_x from the stronger EEP indirect effect is at least partly responsible for the absence of ozone super recovery in the upper stratosphere.

4 Summary

In this paper we show that future scenarios with stronger greenhouse gas forcing lead to overall higher levels of simulated stratospheric ozone. Ozone in SSP5 relative to SSP2 is higher in the upper stratosphere and lower in the equatorial lower stratosphere at the end of the 21st century. These ozone differences are a consequence of different carbon dioxide and methane
140 emissions and the resulting lower temperatures in the middle atmosphere. A cooler stratosphere will increase ozone production, leading to an ozone increase in the upper stratosphere. A negative anomaly in the lower equatorial stratosphere is a consequence of accelerated transport via a stronger Brewer-Dobson circulation. The mesospheric ozone decrease in SSP5 relative to SSP2 is likely a consequence of additional HO_x production from higher methane emissions in SSP5.

In SSP3 and SSP5, ozone will have a super recovery in the Arctic stratosphere and Antarctic lower stratosphere towards
145 2100. However, ozone in the Antarctic upper stratosphere have similar levels across the different future scenarios which are not above the pre-CFC levels at the end of the 21st century. We show that this is due to excess NO_x descending from the mesosphere in the stronger scenarios and the resulting catalytic ozone loss. This NO_x is produced in the thermosphere and the upper mesosphere by energetic electron precipitation and descends faster in future scenarios with higher greenhouse gas forcing (Maliniemi et al., 2020).

150 It is clear that stratospheric ClO_x will decrease in the future, following the adoption of the Montreal protocol (Velders et al., 2007). As a result, the catalytic NO_x cycle is more important for ozone variability in the future. EEP is an important source of mesospheric and stratospheric NO_x , especially following winter darkness when its chemical lifetime is long. Furthermore, the EEP indirect effect is becoming stronger in the southern hemisphere under higher greenhouse gas forcing (Maliniemi et al., 2020). This places energetic electron precipitation as an element with increasing importance for the future of ozone in the polar
155 stratosphere.

EEP related ozone depletion can potentially influence stratospheric temperatures and the polar vortex (Arsenovic et al., 2016; Salminen et al., 2019; Asikainen et al., 2020). The polar vortex has a notable effect on winter weather in the mid- and high latitudes (Thompson and Solomon, 2002; Kidston et al., 2015). Thus, there is a great potential of improving future projections (not only to ozone) and seasonal forecasts of polar regions by implementing EEP forcing to the earth system models (Matthes
160 et al., 2017).

Data availability. WACCM simulations used in this study are available as part of the CMIP6 on the Earth System Grid (<https://esgf-node.llnl.gov/projects/cmip6/>).



Author contributions. D.R.M provided the WACCM model outputs. V.M analysed the data and wrote the manuscript. All authors contributed to the analyses of the results and modification of the manuscript.

165 *Competing interests.* The authors declare no competing interest.

Acknowledgements. We thank the National Center for Atmospheric Research for WACCM model outputs. The research has been funded by the Norwegian Research Council under Contracts 223252/F50 (BCSS) and 300724 (EPIC). The National Center for Atmospheric Research is sponsored by the National Science Foundation.



References

- 170 Anderson, J. G., Toohey, D. W., and Brune, W. H.: Free radicals within the Antarctic vortex: the role of CFCs in Antarctic ozone loss, *Science*, 251, 39–46, <https://doi.org/10.1126/science.251.4989.39>, 1991.
- Andersson, M. E., Verronen, P. T., Marsh, D. R., Seppälä, A., Päivärinta, S., Rodger, C. J., Clilverd, M. A., Kalakoski, N., and van de Kamp, M.: Polar ozone response to energetic particle precipitation over decadal time scales: the role of medium-energy electrons, *J. Geophys. Res. Atmos.*, 123, <https://doi.org/10.1002/2017JD027605>, 2018.
- 175 Arsenovic, P., Rozanov, E., Stenke, A., Funke, B., Wissing, J. M., Mursula, K., Tummon, F., and Peter, F.: The influence of middle range energy electrons on atmospheric chemistry and regional climate, *J. Atmos. Sol.-Terr. Phys.*, 149, 180–190, <https://doi.org/10.1016/j.jastp.2016.04.008>, 2016.
- Asikainen, T., Salminen, A., Maliniemi, V., and Mursula, K.: Influence of enhanced planetary wave activity on the polar vortex enhancement related to energetic electron precipitation, *J. Geophys. Res. Atmos.*, 125, e2019JD032137, <https://doi.org/10.1029/2019JD032137>, 2020.
- 180 Baumgaertner, A. J. G., Jöckel, P., Dameris, M., and Crutzen, P. J.: Will climate change increase ozone depletion from low-energy-electron precipitation?, *Atmos. Chem. Phys.*, 10, <https://doi.org/10.5194/acp-10-9647-2010>, 2010.
- Brasseur, G. P. and Solomon, S.: *Aeronomy of the middle atmosphere*, Springer, 2005.
- Butchart, N.: The Brewer-Dobson circulation, *Rev. Geophys.*, 52, 157–184, <https://doi.org/10.1002/2013RG000448>, 2014.
- Cicerone, R. J.: Changes in stratospheric ozone, *Science*, 237, 35–42, <https://doi.org/10.1126/science.237.4810.35>, 1987.
- 185 Cleveland, W. S. and Devlin, S. J.: Locally-weighted regression: an approach to regression analysis by local fitting, *J. Am. Stat. Assoc.*, 83, <https://doi.org/10.2307/2289282>, 1988.
- Funke, B., López-Puertas, M., Stiller, G. P., and Clarmann, T.: Mesospheric and stratospheric NO_y produced by energetic particle precipitation during 2002–2012, *J. Geophys. Res.*, 119, <https://doi.org/10.1002/2013JD021404>, 2014.
- Garcia, R. R. and Randel, W. J.: Acceleration of the Brewer–Dobson circulation due to increases in greenhouse gases, *J. Atmos. Sci.*, 65, 2731–2739, <https://doi.org/10.1175/2008JAS2712.1>, 2008.
- 190 Gettelman, A., Hannay, C., Bacmeister, J. T., Neale, R. B., Pendergrass, A. G., Danabasoglu, G., Lamarque, J.-F., Fasullo, J. T., Bailey, D. A., Lawrence, D. M., and Mills, M. J.: High climate sensitivity in the community earth system model version 2 (CESM2), *Geophys. Res. Lett.*, 46, <https://doi.org/10.1029/2019GL083978>, 2019.
- Kidston, J., Scaife, A. A., Hardiman, S. C., Mitchell, D. M., Butchart, N., Baldwin, M. P., and Gray, L. J.: Stratospheric influence on tropospheric jet streams, storm tracks and surface weather, *Nature Geosci.*, 8, 433–440, <https://doi.org/10.1038/ngeo2424>, 2015.
- 195 Kirner, O., Ruhnke, R., and Sinnhuber, B.-M.: Chemistry–climate interactions of stratospheric and mesospheric ozone in EMAC long-term simulations with different boundary conditions for CO₂, CH₄, N₂O, and ODS, *Atmosphere-Ocean*, 53, 140–152, <https://doi.org/10.1080/07055900.2014.980718>, 2015.
- Langematz, U.: Future ozone in a changing climate, *Comptes Rendus Geoscience*, 350, 403 – 409, <https://doi.org/https://doi.org/10.1016/j.crte.2018.06.015>, 2018.
- 200 le Texier, H., Solomon, S., and Garcia, R. R.: The role of molecular hydrogen and methane oxidation in the water vapour budget of the stratosphere, *Q. J. Roy. Meteor. Soc.*, 114, 281–295, <https://doi.org/https://doi.org/10.1002/qj.49711448002>, 1988.
- Li, F., Stolarski, R. S., and Newman, P. A.: Stratospheric ozone in the post-CFC era, *Atmos. Chem. Phys.*, 9, 2207–2213, <https://doi.org/10.5194/acp-9-2207-2009>, 2009.



- 205 Maliniemi, V., Marsh, Daniel, R., Tyssøy, H. N., and Smith-Johnsen, C.: Will climate change impact polar NO_x produced by energetic particle precipitation?, *Geophys. Res. Lett.*, 47, e2020GL087041, <https://doi.org/https://doi.org/10.1029/2020GL087041>, 2020.
- Marsh, D. R., Mills, M. J., Kinnison, D. E., Lamarque, J.-F., Calvo, N., and Polvani, L. M.: Climate change from 1850 to 2005 simulated in CESM1(WACCM), *J. Climate*, 26, <https://doi.org/10.1175/JCLI-D-12-00558.1>, 2013.
- Matthes, K., Funke, B., Anderson, M., Barnard, L., Beer, J., Charbonneau, P., Clilverd, M., Dudok de Wit, T., Haberreiter, M., Hendry, A., Jackman, C., Kretschmar, M., Kruschke, T., Kunze, M., Langematz, U., Marsh, D., Maycock, A., Misios, S., Rodger, G., Scaife, A., Seppälä, A., Shangguan, M., Sinnhuber, M., Tourpali, K., Usoskin, I., van de Kamp, M., Verronen, P., and Versick, S.: Solar forcing for CMIP6 (v3.1), *Geosci. Model Dev.*, 10, <https://doi.org/10.5194/gmd-10-2247-2017>, 2017.
- 210 Meinshausen, M., Nicholls, Z. R. J., Lewis, J., Gidden, M. J., Vogel, E., Freund, M., Beyerle, U., Gessner, C., Nauels, A., Bauer, N., Canadell, J. G., Daniel, J. S., John, A., Krummel, P. B., Luderer, G., Meinshausen, N., Montzka, S. A., Rayner, P. J., Reimann, S., Smith, S. J., van den Berg, M., Velders, G. J. M., Vollmer, M. K., and Wang, R. H. J.: The shared socio-economic pathway (SSP) greenhouse gas concentrations and their extensions to 2500, *Geosci. Model Dev.*, 13, 3571–3605, <https://doi.org/10.5194/gmd-13-3571-2020>, 2020.
- 215 Mitchell, D. M., Osprey, S. M., Gray, L. J., Butchart, N., Hardiman, S. C., Charlton-Perez, A. J., and Watson, P.: The effect of climate change on the Variability of the northern hemisphere stratospheric polar vortex, *J. Atmos. Sci.*, 69, 2608 – 2618, <https://doi.org/10.1175/JAS-D-12-021.1>, 2012.
- 220 O’Neill, B. C., Tebaldi, C., van Vuuren, D. P., Eyring, V., Friedlingstein, P., Hurtt, G., Knutti, R., Kriegler, E., Lamarque, J.-F., Lowe, J., Meehl, G. A., Moss, R., Riahi, K., and Sanderson, B. M.: The scenario model intercomparison project (ScenarioMIP) for CMIP6, *Geosci. Model Dev.*, 9, <https://doi.org/10.5194/gmd-9-3461-2016>, 2016.
- Randall, C. E., Harvey, V. L., Singleton, C. S., Bernath, P. F., Boone, C. D., and Kozyra, J. U.: Enhanced NO_x in 2006 linked to strong upper stratospheric Arctic vortex, *Geophys. Res. Lett.*, 33, <https://doi.org/10.1029/2006GL027160>, 2006.
- 225 Riahi, K., van Vuuren, D. P., Kriegler, E., Edmonds, J., O’Neill, B. C., Fujimori, S., Bauer, N., Calvin, K., Dellink, R., Fricko, O., Lutz, W., Popp, A., Cuaresma, J. C., KC, S., Leimbach, M., Jiang, L., Kram, T., Rao, S., Emmerling, J., Ebi, K., Hasegawa, T., Havlik, P., Humpenöder, F., Silva, L. A. D., Smith, S., Stehfest, E., Bosetti, V., Eom, J., Gernaat, D., Masui, T., Rogelj, J., Strefler, J., Drouet, L., Krey, V., Luderer, G., Harmsen, M., Takahashi, K., Baumstark, L., Doelman, J. C., Kainuma, M., Klimont, Z., Marangoni, G., Lotze-Campen, H., Obersteiner, M., Tabeau, A., and Tavoni, M.: The shared socioeconomic pathways and their energy, land use, and greenhouse gas emissions implications: An overview, *Glob. Environ. Chang.*, 42, <https://doi.org/https://doi.org/10.1016/j.gloenvcha.2016.05.009>, 2017.
- 230 Salminen, A., Asikainen, T., Maliniemi, V., and Mursula, K.: Effect of energetic electron precipitation on the northern polar vortex: explaining the QBO modulation via control of meridional circulation, *J. Geophys. Res. Atmos.*, 124, <https://doi.org/10.1029/2018JD029296>, 2019.
- Shepherd, T. G.: Dynamics, stratospheric ozone, and climate change, *Atmosphere-Ocean*, 46, 117–138, <https://doi.org/10.3137/ao.460106>, 2008.
- 235 Solomon, S., Ivy, D. J., Kinnison, D., Mills, M. J., Neely, R. R., and Schmidt, A.: Emergence of healing in the Antarctic ozone layer, *Science*, 353, <https://doi.org/10.1126/science.aae0061>, 2016.
- Stolarski, R. S., Douglass, A. R., Oman, L. D., and Waugh, D. W.: Impact of future nitrous oxide and carbon dioxide emissions on the stratospheric ozone layer, *Environ. Res. Lett.*, 10, <https://doi.org/10.1088/1748-9326/10/3/034011>, 2015.
- Thompson, D. W. J. and Solomon, S.: Interpretation of recent southern hemisphere climate change, *Science*, 296, 895–899, <https://doi.org/10.1126/science.1069270>, 2002.
- 240 Velders, G. J. M., Andersen, S. O., Daniel, J. S., Fahey, D. W., and McFarland, M.: The importance of the Montreal Protocol in protecting climate, *Proc. Natl. Acad. Sci.*, 104, <https://doi.org/10.1073/pnas.0610328104>, 2007.



- Wilks, D. S.: “The stippling shows statistically significant grid points”: how research results are routinely overstated and overinterpreted, and what to do about it, *Bull. Am. Meteorol. Soc.*, 97, <https://doi.org/10.1175/BAMS-D-15-00267.1>, 2016.
- 245 WMO: Scientific assessment of ozone depletion: 2018, Global Ozone Research and Monitoring Project – Report No. 58, 588 pp., Geneva, Switzerland, 2018.